Microchemical Journal 117 (2014) 40–45

Contents lists available at ScienceDirect

Microchemical Journal

journal homepage: www.elsevier.com/locate/microc

Multivariate optimization of a solid phase extraction system employing L-tyrosine immobilized on carbon nanotubes applied to molybdenum analysis by inductively coupled plasma optical emission spectrometry with ultrasound nebulization

Cristian Bazán [a], Raúl Gil [a], Patricia Smichowski [b], Pablo Pacheco [a,*]

[a] Instituto de Química de San Luis (INQUISAL-CONICET), Chacabuco y Pedernera, CP 5700 San Luis, Argentina
[b] Comisión Nacional de Energía Atómica, Gerencia Química, Av. Gral. Paz 1499, B1650KNA-San Martín, Pcia, Buenos Aires, Argentina

ARTICLE INFO

Article history:
Received 14 May 2014
Received in revised form 4 June 2014
Accepted 6 June 2014
Available online 14 June 2014

Keywords:
Molybdenum
L-tyrosine
Carbon nanotubes
Multivariate optimization

ABSTRACT

A method for Mo solid phase extraction on L-tyrosine immobilized on carbon nanotubes (L-tyr-CNTs) is presented. L-tyr-CNTs were used to fill a minicolumn and introduced into a FI system employing inductively coupled plasma optical emission spectrometry with ultrasound nebulization (USN-ICP OES). Five FI parameters such as buffer flow rate (BFR) and concentration (BC); sample flow rate (SFR); eluent flow rate (EFR) and concentration (EC); and pH were chosen for optimization employing a half fraction composite design (HFFD). Multivariate optimization through central composite design (CCD) allowed establishing the statistical ideal parameter values to reach maximum Mo signal. From HFFD and CCD it was established that SFR was not affecting the system significantly and that the optimal experimental conditions were: pH, 4.0; BC, 5 mM ammonium acetate; EC, 15% (v v^{-1}) and EFR, 2 mL min^{-1}. Under these conditions an enhancement factor of 750-fold (25 for preconcentration system and 30 for USN) was obtained reaching a detection limit of 40 ng L^{-1} with a precision of 1.32%. The system was successfully applied to a certified reference material NIST CRM 1643e (trace elements in water) and river, thermal, mine and tap water samples.

1. Introduction

The transition element molybdenum is an essential micronutrient for microorganisms, plants, and animals and is one of the ten biologically active elements [1]. Molybdenum (Mo) is the only second-row transition metal with biological activity. Among the existing compounds of Mo in nature, oxyanion molybdate (MoO_4^{2-}) is the predominant form in solution at pH higher than 4.2, and therefore cells take up Mo from the external medium in the form of molybdate [2].

Mo is present in low and diverse amounts in continental (5 nmol L^{-1}) and marine (100 nmol L^{-1}) waters, and in soils (1.1 mg kg^{-1}) [3–5]. In biological tissues, Mo is one of the scarcest elements. In human serum, molybdenum concentration lower than 1 μg L^{-1} was reported [6], while mean concentration in urine was 42.5 μg L^{-1} [7]. In contrast, many elements that are present in considerably larger amounts have no apparent biological function (e.g., Al, Ti, or Zr) [8]. These low Mo concentrations in environmental and biological samples, along with the high concentration of interfering matrix components, require sensitive instrumentation to reach its determination.

In this sense ICP OES has been applied to molybdenum determination [9]. Despite the fact that it has been used by a good number of researchers, it does not posses the necessary sensitivity for trace and ultra-trace analysis, and the use of a separation–preconcentration procedure is inevitable [10]. Spectral interferences in Mo determination by ICP-OES have been reported. Baucells et al. [11] reported the spectral interference of aluminium and magnesium and Dos Santos et al. [12] noted the spectral interference of aluminium, magnesium, and iron in Mo determination. For all the aforementioned considerations, determination of trace amounts of Mo using ICP-OES is almost always preceded by a previous pre-concentration step, using separation techniques [13].

Among the methods reported for preconcentration and matrix separation of molybdenum, sorbent extraction has proved to be especially effective [14]. Nowadays, carbon nanotubes (CNTs) have been proposed as a novel solid phase extractant for metal ions [15]. The hexagonal arrays of carbon atoms in graphite sheets of CNTs' surface are ideal for strong interactions with other molecules. The large surface areas of CNTs make them a promising solid sorbent for preconcentration procedures. In addition a proper surface treatment of CNTs can improve metal sorption and selectivity in SPE [16]. In this context different amino acids have been immobilized on CNTs for metal retention like L-tyrosine [17,18].

* Corresponding author. Tel.: +54 266 4446765.
E-mail address: ppacheco@unsl.edu.ar (P. Pacheco).

http://dx.doi.org/10.1016/j.microc.2014.06.003
0026-265X/

The introduction of on-line systems to solid phase extraction (SPE) systems provides the possibility of automation which increases precision and accuracy [19]. However an on-line system requires optimization of several variables leading to a tedious and time consuming work. As an alternative, multivariate techniques have been introduced for analytical method optimization [20]. These techniques allow several variables to be optimized simultaneously representing several advantages, such as speed of analysis, practicality, economy, and reduction in the number of experiments that need to be carried out [21]. In addition, these methods are able to generate mathematical models that estimate the relevance as well as statistical significance of the factors' effects on the processes and also evaluate the interactions' effects among the factors. Factorial design is one of the mathematical models for multivariate optimization and is widely applied in chemistry. In order to determine the real functionality established among the analytical response and the significant factors, second order designs eventually are also necessary.

The present research introduces L-tyr immobilized on carbon nanotubes (L-tyr-CNTs) as an alternative for Mo retention and preconcentration. To this end L-tyr-CNTs were packed in a minicolumn and introduced into an FI system employing USN-ICP OES as detection system. A two-level fractional factorial design was used to evaluate the experimental variables including buffer flow rate and concentration; sample flow rate; acid flow rate and concentration; and pH. The experiments for the final system optimization were performed according to the central composite response surface experimental design. The system was successfully applied to Mo determination in QC-LL2 standard reference material (metals in natural water) and different water samples.

2. Experimental

2.1. Instrumentation

Measurements were performed with a sequential ICP spectrometer Baird ICP 2070 (Bedford, MA, USA.). The 1 m Czerny–Turner monochromator had a holographic grating with 1800 grooves mm^{-1}. The FI system used is shown in Fig. 1. An ultrasonic nebulizer, U 5000 AT [CETAC Technologies (Omaha, NE, USA)], with desolvation system was used. The ICP and ultrasonic nebulizer operating conditions are listed in Table 1. A Minipulse 3 peristaltic pump Gilson (Villiers-Le-Bell, France) was used. Sample injection was achieved using a Rheodyne (Cotati, CA, USA) Model 50, four-way and of 6 ports, 2 positions, rotary valves. The conical minicolumn was prepared by placing 25 mg of L-tyr-CNTs into an empty conical tip using the dry packing method. To avoid loss of filling when the sample solution passed through the conical minicolumn, a small amount of quartz wool was placed at both ends of conical minicolumn. The column was then connected to a peristaltic pump with PTFE tubing to form the preconcentration system. Tygon type pump tubing (Ismatec, Cole Parmer, Vernon Hills, IL, USA) was employed to propel the sample, reagents and eluent. The Mo 202.030 nm spectral line was used.

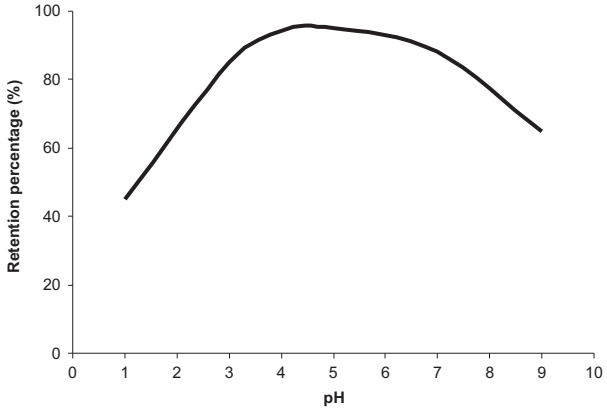

Fig. 1. Dependence of Mo retention on pH of loading solutions. Volume of sample: 10 mL; Mo (VI) concentration: 1 mg L^{-1}; eluent concentration: 10.0% (v/v).

Table 1
ICP and ultrasonic nebulizer instrumental parameters.

ICP conditions	
RF generator power plasma	0.8 kW
Frequency of RF generator	40.68 MHz
Gas flow rate	8.5 L min^{-1}
Auxiliary gas flow rate	1 L min^{-1}
Observation height-above load coil.	15 mm
Analytical line	Mo 202.030 nm
Ultrasonic nebulizer conditions	
Heater temperature	140 °C
Condenser temperature	4.0 °C
Carrier gas flow rate	1 L min^{-1}

2.2. Reagents

Unless otherwise stated, the chemicals used were of analytical grade, and therefore no further purification was required. A molybdenum stock solution (1000 mg L^{-1}) was prepared by dissolving 920.3 mg $(NH_4)_6Mo_7O_{24}\cdot 4H_2O$ in water and the volume was filled up to 500 mL with water and a few drops of concentrated nitric acid (Fluka). Commercial multiwall CNTs were obtained from Sunnano (Jiangxi, China). L-Tyrosine was obtained form MP Biomedicals Inc. (Chicago, IL, USA).

2.3. Sample collection

Mine water samples were obtained from La Carolina (San Luis, Argentina) abandoned mine. River water samples were obtained from Conlara River (San Luis, Argentina) and Quinto River (San Luis–Córdoba, Argentina). Thermal water samples were obtained from San Gerónimo (San Luis, Argentina) pools. Tap water samples were obtained directly from San Luis City (Argentina) water system. Immediately after collection, samples were filtered through 0.45 μm pore size membrane filters, acidified with nitric acid, and stored at 4 °C in Nalgene bottles.

The method accuracy was checked by applying it to Mo determination in the standard reference material NIST CRM 1643e (Trace Elements in Water).

2.4. Immobilization procedure

About 50 mg of commercial multiwall CNTs were treated with concentrated HNO_3 to clean them and eliminate possible Mo residues present in CNTs since metallic impurities are inherently present in CNT samples because CNTs are typically synthesized by using metallic (typically Fe, Ni, Co, Mo) catalyst nanoparticles [22]. This procedure also allowed the generation of –COOH and –OH groups on CNTs' surface, improving their solubility [23]. After this, CNTs were centrifuged, filtrated and dried.

The resultant powder was suspended in phosphate buffer pH 7.0 and an aliquot of 50 mg of the amino acid (L-tyr) was added to the buffer solution. After this, the solution was heated for 48 h at 45 °C. Finally, it was filtered, and CNTs were dried at room temperature.

2.5. Procedure

The flow injection system used for preconcentration, separation and subsequent determination of Mo has been reported before [24,25]. Before loading, the column was conditioned for preconcentration at the

optimized pH. A volume of sample was then loaded on the conical-minicolumn at flow rate of 10 mL min^{-1}. Finally, the molybdenum retained was eluted with a 20% (v/v) nitric acid solution. After that, it was introduced directly into the USN unit and subsequently to ICP torch. The operation conditions were established and determination was carried out.

2.6. Optimization strategy

The optimization process was accomplished using a half-fraction factorial design and a central composite design (CCD). All the experiments run in duplicate using 1 mg L^{-1} Mo (VI) solution. Five variables were studied: sample flow rate (SFR), eluent flow rate (EFR), eluent concentration (EC), buffer concentration (BC) and pH. Experimental design, data analysis and desirability function calculations were performed by using the software Stat-Ease Design-Expert trial Version 8.0.

2.6.1. Screening phase: half-fraction factorial design (HFFD)

Experimental half-fraction factorial design is a factorial analysis involving ½ of the number of experiments of the full factorial design. This may be successfully applied with the aim to determine which variables mainly influence Mo retention on L-tyr-CNTs. Moreover, a good experimental design provides a simple, efficient, and systematic approach to optimize designs for performance, quality and cost. A duplicate two-level factorial design with $2 \times 2^{(5-1)} = 32$ experiments (Table 2) is described here for the variables: buffer flow rate (BFR) and concentration (BC); sample flow rate (SFR); eluent flow rate (EFR) and concentration (EC); and pH.

2.6.2. Optimization phase: central composite design (CCD)

Systematic optimization procedures are carried out by selecting an objective function, finding the most important factors and investigating the relationship between responses and factors by the so-called response surface methods (RSM). In the common way, a simple response is analyzed, and the model analysis indicates areas in the design region where the process is likely to give desirable results [29].

Once the conditions that ensure maximum Mo retention were established, a spherical CCD was used here consisting of 30 experiments; i.e. combinations of 4 factorial points, 4 axial points, and 6 replicates of a central point. The studied levels were selected considering the results of the HFFD.

All experiments were performed in random order to minimize the effects of uncontrolled factors that may introduce bias in the measurements.

Table 2
Half design built for factor selection.

Experiment	SFR[a]	pH	BF[a]	EC[a]	EFR[a]	RAS[a]
1	2	6	5	5	2	25.00
2	2	4	15	15	3	16.60
3	2	4	15	5	2	34.30
4	4	4	5	5	2	34.29
5	4	4	5	15	3	31.40
6	2	4	5	15	2	46.53
7	2	4	15	5	2	100.00
8	4	4	5	15	3	27.66
9	4	4	15	15	2	31.23
10	4	6	5	5	3	18.92
11	4	6	5	15	2	34.46
12	4	6	15	5	2	24.52
13	2	6	15	5	3	24.58
14	4	6	15	15	3	19.41
15	2	4	5	5	3	57.06
16	2	6	15	5	3	19.28
17	2	4	5	15	2	81.88
18	4	4	15	5	3	47.92
19	2	6	15	15	2	24.55
20	4	6	5	5	3	25.49
21	2	6	5	15	3	23.92
22	4	6	5	15	2	31.04
23	4	4	5	5	2	40.67
24	2	6	5	5	2	25.85
25	2	6	15	15	2	21.19
26	4	4	15	5	3	42.75
27	2	4	5	5	3	44.16
28	2	4	15	15	3	44.73
29	4	6	15	15	3	14.30
30	4	6	15	5	2	18.97
31	2	6	5	15	3	22.05
32	4	4	15	15	2	46.48

[a] SFR: sample flow rate; BF: buffer concentration; EC: eluent concentration; EFR: eluent flow rate; RAS: relative analytical response.

3. Results and discussion

3.1. Preliminary studies: pH effect

As mentioned previously, Mo working standard solution was prepared with a Mo^{6+} salt, $[(NH_4)_6Mo_7O_{24}\cdot 4H_2O]$. Considering the amino acid immobilized on CNTs, L-tyrosine, there is evidence for bidentate coordination of amino acids and Mo through one carboxyl oxygen atom and the amino-nitrogen [26]. In addition, since L-tyrosine has phenol as side chain-group (R-group), it has been stated that alcoholic oxygen atom and one phenolic oxygen atom may be involved in the formation of molybdenum dioxo complexes as well [27].

In Fig. 1 Mo retention on L-tyr-CNTs according to pH can be observed. At low pH values (<2.0) retention is not quantitative since Mo^{6+} species are protonated [28]. As pH increases, Mo retention percentage increases accordingly with Mo deprotonation and oxyanion formation. When the alkaline region in the pH range begins, Mo retention decreases reaching a minimum at pH values close to 10.0, coincident with L-tyrosine side chain deprotonation (pKa = 10.5) [29]. For future studies a pH range of 3.00–7.00 was selected for optimization studies.

3.2. Half-fraction factorial design (HFFD)

L-tyr-CNTs have been already employed for elemental [18] and elemental species determination [17] as sorbent in SPE systems. It has been described that pH, eluent flow rate (EFR) and concentration (EC) and sample flow rate (SFR) are parameters governing the retention dynamics. Accordingly these parameters were chosen for optimization. Since pH can be accurately controlled employing a buffer solution, ammonium acetate was chosen as buffer and its concentration (BC) was include as parameter for optimization.

Since many variables are involved in Mo retention efficiency by L-tyr-CNTs it is important to elucidate which of these variables are significantly affecting the system. In this sense HFFD arises as a valuable statistical tool to clarify this matter. These factors were evaluated at two levels each as discussed above (Table 2). The evaluation consisted in analyzing stock standard solutions in all cited conditions. Analysis of variance (ANOVA) and *p*-value were used to evaluate the significance ($p < 0.05$) of the effects, main effects and their interactions on the SPE system as depicted in the Pareto chart shown in Fig. 2 (ANOVA Table included as Supplementary Electronic Material). There are 4 factors that significantly affect the retention system (negative effects): **B**, pH ($p < 0.0001$); **C**, BC ($p = 0.0026$); **D**, EC ($p = 0.0424$) and **E**, EFR ($p = 0.0346$). Only **A**, SFR, did not significantly affect the system ($p = 0.8456$). This point contrasts with previous research where it was stated that the influent concentration affects metal retention on L-tyr-CNTs [18]. However the sample flow rate range evaluated in this work is higher, between 2 and 4 mL min^{-1} and Mo concentrations evaluated are lower, 0.1 mg L^{-1}.

Pareto chart also shows other parameters that have been excluded from HFFD (bars fully colored) since they are not significantly influencing the system. On the other hand, despite not being significant, variable SFR (**A**) was included since AC interaction is significant acquiring hierarchy to be included in further optimization.

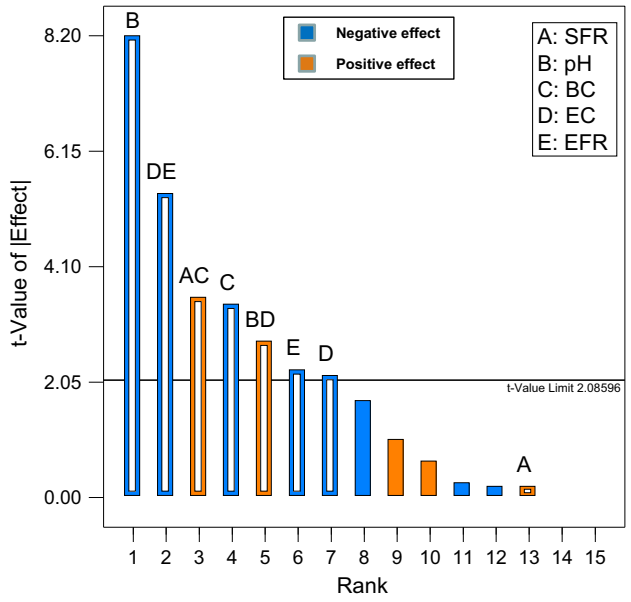

Fig. 2. Pareto chart for the studied effects. Bars fully colored have been excluded from half fraction factorial design. (For interpretation of the references to color in this figure legend, the reader is referred to the web version of this article.)

3.3. Central Composite Design (CCD)

From HFFD 4 variables, pH, BC, EC and EFR, arose as the most significant factors affecting Mo retention on L-tyr-CNTs. In order to reach an interpretation of those effects over the analytical response, a CCD was built through a multilevel design. Table 3 shows the experimental matrix defined for the factors previously selected in the HFFD. The experimental ranges evaluated to obtain the optimal conditions can also be observed.

Table 3
Central composite design.

Experiment	pH	BF[a]	EC[a]	EFR[a]	RAS[a]
1	5	7.5	0	2.5	32.96
2	4	15	5	3	60.59
3	6	5	5	2	43.21
4	5	7.5	7.5	2.5	40.04
5	4	15	5	2	82.10
6	5	7.5	7.5	4	27.82
7	5	7.5	7.5	1	49.97
8	6	5	5	3	62.25
9	5	7.5	7.5	2.5	39.37
10	4	5	5	3	58.75
11	4	15	15	2	64.64
12	6	15	15	2	76.01
13	3	7.5	7.5	2.5	38.99
14	6	5	15	3	48.50
15	5	7.5	1	2.5	35.52
16	5	7.5	7.5	2.5	29.61
17	4	5	15	3	71.76
18	5	7.5	1	2.5	42.29
19	5	7.5	7.5	2.5	45.98
20	6	15	5	3	51.98
21	5	7.5	7.5	2.5	31.87
22	5	19	7.5	2.5	36.65
23	6	15	5	2	75.16
24	6	5	15	2	77.18
25	7	7.5	7.5	2.5	41.90
26	4	15	15	3	68.67
27	4	5	5	2	93.40
28	6	15	15	3	65.99
29	4	5	15	2	100.00
30	5	1	7.5	2.5	45.38

[a] BF: buffer concentration; EC: eluent concentration; EFR: eluent flow rate; RAS: relative analytical.

Fig. 3 shows surface responses of Mo retention as a function of the individual factors under study, while maintaining the others at their optimal values. As mentioned previously, variable **A** (SFR) was included in CCD since AC interaction is significant to the system acquiring **A** hierarchy to be included in optimization. From observation and evaluation of surface graphics from CCD, as general interpretation, Mo retention increases at lower pH, BC, EC and EFR values in the studied range. As expected, SFR or **A** variable shows a slight influence on Mo retention as can be observed in the moderated slope of the edge's surface corresponding to SFR axis.

Optimized experimental conditions corresponding to maximum Mo signal after preconcentration are: pH, 4.0; BC, 5 mM ammonium acetate; EC, 15% ($v\ v^{-1}$) and EFR, 2 mL min^{-1}.

3.4. Analytical performance

After optimization through HFFD and CCD, different analytical parameters were determined to define the performance of the FI-USN-ICP OES system employing L-tyr-CNTs as sorbent for SPE. Under the optimized conditions and preconcentration of 2 mL (1 min at a flow rate of 2 mL min^{-1}), an enrichment factor of 25 was obtained reaching an overall enhancement factor of 750-fold (25 for preconcentration system and 30 for USN) compared with direct Mo determination by ICP OES. A detection limit (LoD) of 40 ng L^{-1} was obtained calculated according to 3σ definition. Precision was calculated as the standard variation of 10 standard measurements and corresponded to 1.32%. Linearity was held until 10 mg L^{-1}.

Table 4 shows a comparison between this research and different approaches reported in literature regard Mo preconcentration employing SPE and FI systems. L-tyr-CNTs show improved features like sample volume, precision and enrichment factor, this last attributed to easily metal released by pH lowering and the presence of the active sites on the surface, inner cavities and inter-nanotube space contributing to the high metal removal capability of CNTs [18]. However L-tyr-CNTs show no improvement in sample flow rate, this can be explained considering the minicolumns clogging observed when nanomaterials are used for SPE. This statement is enforced by comparison of L-tyr-CNTs and nanometer-sized titanium dioxide [30] sample flow rates with the rest ones of the introduced sorbents in Table 4.

3.5. Recovery studies and validation

In order to evaluate the Mo recovery of this method and its suitability for real sample analysis the method was applied to different water samples, detailed in Section 2.3, as follows: ten sample aliquots were divided into 4 aliquots and added with different Mo concentrations as observed in Table 5. Recoveries were between 95.1 and 102.3%.

Mo concentration in water samples from San Luis–Argentina water network corresponds to 0.63 ± 0.010 μg L^{-1}. This value is in good agreement with other studies reported in literature for Mo in tap water. Ensafi et al. reported 0.19 ± 0.02 [31] and 1.06 ± 0.09 [32] μg L^{-1}. In addition Escudero et al. reported 0.88 ± 0.08 μg L^{-1} [24] and Gil et al. reported 0.84 ± 0.02 μg L^{-1} [25] of Mo concentration in tap water. The determined Mo concentration in drinking water samples is below the tolerance limit concentration (80 μg L^{-1}) of molybdenum in drinking water established by the Environmental Protection Agency (EPA), that is not expected to cause any adverse noncarcinogenic effects for up to one day of exposure, intended to protect a 10-kg child consuming 1 L of water per day [33].

Molybdenum was not detected in Conlara River water samples and in Quinto River Mo concentrations of 0.53 ± 0.01 μg L^{-1} were determined. This concentration is in good agreement with those found by Yamaguchi et al. [34] in the eastern area of Shimane Prefecture, Japan near Mo mines. However Mo was not detected in water samples from

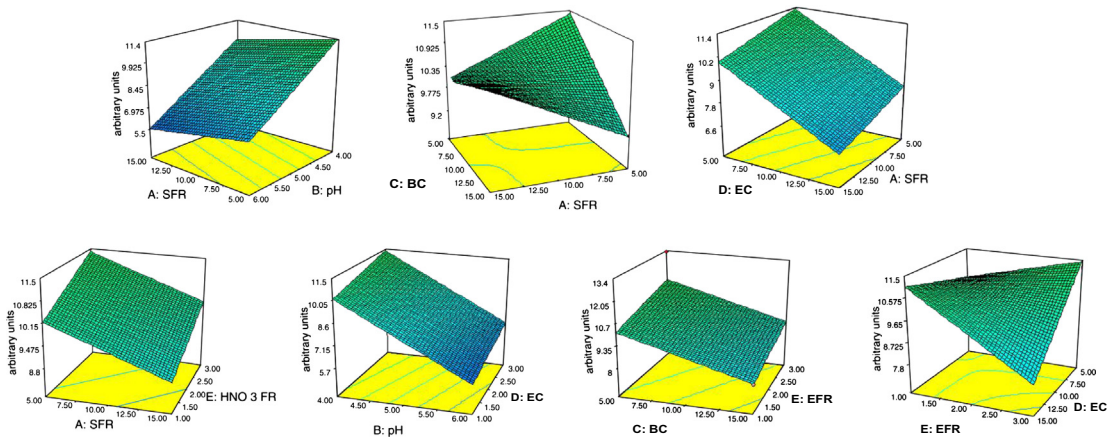

Fig. 3. Response surfaces obtained using central composite design.

Table 4
Comparison of different sorbents efficiency for Mo preconcentration with analytical purposes.

Sorbent	Sample volume (mL)	Sample flow rate (mL min^{-1})	Enrichment factor	Precision (%)	Reference
L-tyr-CNTs	2	2	750	1.32	This work
Dowex 1 − x8 resin	600	5	120	<4	[35]
Metal alkoxide glass immobilized 8-quinolinole	7	3.2	20–30	3.29–8.41	[36]
Immobilized baker's yeasts on controlled pore glass	10	5.0	480	1.9	[25]
Muromac A-1	7	3.5	2.8–13.3	<5.4	[37]
Chitosan resin functionalized with 3,4-dihydroxy benzoic acid	5	1	8–12	0.5–4	[38]
Ethyl vinyl acetate turnings	20	5	300	3.5	[24]
Nanometer-sized titanium dioxide	50–100	1.5	100	1.8	[30]

La Carolina mines. Molybdenum analysis in thermal water showed concentrations of 3.3 ± 0.029 μg L^{-1}. Molybdenum concentrations in thermal water have not been reported in literature.

The accuracy of the proposed method was evaluated by molybdenum determination in a certified reference material NIST CRM 1643e, with a certified value for Mo of 121.4 ± 1.3 μg L^{-1} and a density of 1.016 g mL^{-1} at 22 °C. The determined Mo concentration was of 120.8 ± 1.0 μg L^{-1}, correspondent with the informed value in CRM.

Table 5
Recovery study (95% confidence interval, n = 10).

Sample	Mo added (μg L^{-1})	Mo found (μg L^{-1})[c]	Recovery (%)[a]
Drinking water	0.0	0.63 ± 0.010	–
	0.5	1.14 ± 0.018	100.1
	1.0	1.55 ± 0.025	95.1
	1.5	2.10 ± 0.032	98.6
Conlara River water	0.0	ND[b]	–
	1.0	0.97 ± 0.019	97.7
	2.5	2.53 ± 0.031	101.3
	5.0	4.83 ± 0.059	96.6
Quinto River water	0.0	0.53 ± 0.010	–
	0.5	1.00 ± 0.012	95.9
	1	1.98 ± 0.024	98.7
	1.5	1.50 ± 0.026	100.3
Mine water	0.0	ND[b]	–
	1.0	1.01 ± 0.012	101.9
	2.5	2.42 ± 0.031	96.9
	5.0	4.99 ± 0.064	99.9
Thermal water	0.0	3.30 ± 0.029	–
	1.0	4.29 ± 0.041	99.0
	2.5	6.05 ± 0.061	102.3
	5.0	8.40 ± 0.083	98.5

[a] [(Found-base) / added] * 100.
[b] ND: Non Detected (LoD = 0.04 μg L^{-1}).
[c] Confidence intervals calculated as +/− t(2; 0.05)s / (square root of n).

4. Conclusion

The present research continues demonstrating that the association of amino acids and nanomaterials, in this particular case L-tyr and CNTs, becomes suitable as sorbent for SPE systems. L-tyr and CNTs were successfully introduced into an FI system employing ICP OES with USN as detection for Mo determinations.

Mo retention according to pH revealed that the maximum retention was achieved between 3.00 and 7.00 values coincident with Mo oxyanion formation in aqueous solution. Along with pH, several FI parameters were optimized through a HFFD and CCD like buffer flow rate and concentration; sample flow rate; and eluent flow rate and concentration. From these parameters, only the sample flow rate was not significantly affecting the system.

Multivariate optimization through CCD allowed establishing the statistical ideal parameter values to reach maximum Mo signal. This optimization allowed elevated enrichment factors employing minimal sample volume with precision and accuracy. This last feature was evaluated by CRM analysis and recovery studies of San Luis City drinking water samples, mine water samples from La Carolina (San Luis, Argentina), river water samples from Conlara River (San Luis, Argentina) and Quinto River (San Luis–Córdoba, Argentina) and thermal water samples from San Gerónimo (San Luis, Argentina) pools.

Future studies will continue evaluating the synergy between amino acids' selectivity and CNTs' elevated surface for elemental retention applied to analytical systems.

Supplementary data to this article can be found online at http://dx.doi.org/10.1016/j.microc.2014.06.003.

Acknowledgments

This work was supported by the Consejo Nacional de Investigaciones Científicas y Técnicas (CONICET), Agencia Nacional de Promoción Científica y Tecnológica (FONCYT) (PICTBID), Universidad Nacional de

San Luis (Argentina) and Comisión Nacional de Energía Atómica (CNEA).

References

[1] G. Schwarz, R.R. Mendel, M.W. Ribbe, Molybdenum cofactors, enzymes and pathways, Nature 460 (2009) 839–847.
[2] M. Tejada-Jiménez, A. Chamizo-Ampudia, A. Galván, E. Fernández, Á. Llamas, Molybdenum metabolism in plants, Metallomics 5 (2013) 1191–1203.
[3] B.N. Kaiser, K.L. Gridley, J.N. Brady, T. Phillips, S.D. Tyerman, The role of molybdenum in agricultural plant production, Ann. Bot. 96 (2005) 745–754.
[4] J.M. Martin, M. Meybeck, Elemental mass-balance of material carried by major world rivers, Mar. Chem. 7 (1979) 173–206.
[5] D. Wang, Redox chemistry of molybdenum in natural waters and its involvement in biological evolution, Front. Microbiol. 3 (2012).
[6] P. Schramel, I. Wendler, Molybdenum determination in human serum (plasma) by ICP-MS coupled to a graphite furnace, Fresenius J. Anal. Chem. 351 (1995) 567–570.
[7] B.S. Iversen, C. Menné, M.A. White, J. Kristiansen, J.M. Christensen, E. Sabbioni, Inductively coupled plasma mass spectrometric determination of molybdenum in urine from a Danish population, Analyst 123 (1998) 81–85.
[8] K. Hans Wedepohl, The composition of the continental crust, Geochim. Cosmochim. Acta 59 (1995) 1217–1232.
[9] L.C. Azeredo, M.A.A. Azeredo, R.N. Castro, M.F.C. Saldanha, D.V. Perez, Separation and determination of molybdenum by inductively coupled plasma optical emission spectrometry using quercetin immobilization on silica gel, Spectrochim. Acta B At. Spectrosc. 57 (2002) 2181–2185.
[10] R. Falciani, E. Novaro, M. Marchesini, M. Gucciardi, Multi-element analysis of soil and sediment by ICP-MS after a microwave assisted digestion method, J. Anal. At. Spectrom. 15 (2000) 561–565.
[11] M. Baucells, G. Lacort, M. Roura, Determination of cadmium and molybdenum in soil extracts by graphite furnace atomic-absorption and inductively coupled plasma spectrometry, Analyst 110 (1985) 1423–1429.
[12] H.C. Dos Santos, M.G.A. Korn, S.L.C. Ferreira, Enrichment and determination of molybdenum in geological samples and seawater by ICP-AES using calmagite and activated carbon, Anal. Chim. Acta. 426 (2001) 79–84.
[13] S.L.C. Ferreira, H.C. dos Santos, A.C.S. Costa, M. de la Guardia, Procedures of separation and preconcentration for molybdenum determination using atomic spectrometry — a review, Appl. Spectrosc. Rev. 39 (2004) 457–474.
[14] V. Camel, Solid phase extraction of trace elements, Spectrochim. Acta B At. Spectrosc. 58 (2003) 1177–1233.
[15] M. Tuzen, K.O. Saygi, M. Soylak, Solid phase extraction of heavy metal ions in environmental samples on multiwalled carbon nanotubes, J. Hazard. Mater. 152 (2008) 632–639.
[16] R. Sitko, B. Zawisza, E. Malicka, Modification of carbon nanotubes for preconcentration, separation and determination of trace-metal ions, TrAC Trends Anal. Chem. 37 (2012) 22–31.
[17] P.H. Pacheco, R.A. Gil, P. Smichowski, G. Polla, L.D. Martinez, L-tyrosine immobilized on multiwalled carbon nanotubes: a new substrate for thallium separation and speciation using stabilized temperature platform furnace-electrothermal atomic absorption spectrometry, Anal. Chim. Acta. 656 (2009) 36–41.
[18] P.H. Pacheco, P. Smichowski, G. Polla, L.D. Martinez, Solid phase extraction of Co ions using L-tyrosine immobilized on multiwall carbon nanotubes, Talanta 79 (2009) 249–253.
[19] J. Wang, E.H. Hansen, On-line sample-pre-treatment schemes for trace-level determinations of metals by coupling flow injection or sequential injection with ICP-MS, TrAC Trends Anal. Chem. 22 (2003) 836–846.
[20] M.A. Bezerra, R.E. Santelli, E.P. Oliveira, L.S. Villar, L.A. Escaleira, Response surface methodology (RSM) as a tool for optimization in analytical chemistry, Talanta 76 (2008) 965–977.
[21] S.L.C. Ferreira, W.N.L. Dos Santos, C.M. Quintella, B.B. Neto, J.M. Bosque-Sendra, Doehlert matrix: a chemometric tool for analytical chemistry — review, Talanta 63 (2004) 1061–1067.
[22] M. Giovanni, A. Ambrosi, M. Pumera, Direct determination of bioavailable molybdenum in carbon nanotubes, Chem. Eur. J. 17 (2011) 1806–1810.
[23] P. Liang, E. Zhao, Q. Ding, D. Du, Multiwalled carbon nanotubes microcolumn preconcentration and determination of gold in geological and water samples by flame atomic absorption spectrometry, Spectrochim. Acta B At. Spectrosc. 63 (2008) 714–717.
[24] L. Escudero, R.A. Gil, J.A. Gásquez, R.A. Olsina, L.D. Martínez, Trace molybdenum determination in drinking waters by USN-ICP-OES after solid phase extraction on ethyl vinyl acetate turnings-packed minicolumn, At. Spectrosc. 29 (2008) 21–26.
[25] R.A. Gil, S. Pasini-Cabello, A. Takara, P. Smichowski, R.A. Olsina, L.D. Martínez, A novel on-line preconcentration method for trace molybdenum determination by USN–ICP OES with biosorption on immobilized yeasts, Microchem. J. 86 (2007) 156–160.
[26] R.J. Butcher, H.K.J. Powell, C.J. Wilkins, S.H. Yong, New amino-acid complexes of molybdenum-(V) and -(VI), J. Chem. Soc. Dalton Trans. (1976) 356–359.
[27] A. Syamal, M.A.B.. Niazi, Molybdenum complexes of biochemical interest. New coordination complexes of oxomolybdenum(V) with the tridentate ONO donor schiff bases derived from salicylaldehydes and ethanolamine, Transition Met. Chem. 10 (1985) 54–56.
[28] F.B. Martí, Química Analítica Cualitativa, Thomson, 2002.
[29] M. Campbell, S. Farrell, Biochemistry, Cengage Learning, 2011.
[30] P. Liang, Y. Liu, L. Guo, Determination of molybdenum in steel samples by ICP-AES after separation and preconcentration using nanometre-sized titanium dioxide, J. Anal. At. Spectrom. 19 (2004) 1006–1009.
[31] A.A. Ensafi, T. Khayamian, M. Atabati, Simultaneous voltammetric determination of molybdenum and copper by adsorption cathodic differential pulse stripping method using a principal component artificial neural network, Talanta 57 (2002) 785–793.
[32] A.A. Ensafi, S.S. Khaloo, Determination of traces molybdenum by catalytic adsorptive stripping voltammetry, Talanta 65 (2005) 781–788.
[33] O.o. Water, Edition of the Drinking Water Standards and Health Advisories, in: E.P. Agency (ed.), 2012, (Washington, DC).
[34] T. Yamaguchi, Y. Seike, M. Okumura, On-site solid phase extraction for determination of trace molybdenum in river water samples by graphite furnace atomic absorption spectrometry, Bunseki Kagaku 63 (2014) 59–64.
[35] P.N. Nomngongo, J.C. Ngila, J.N. Kamau, T.A.M. Msagati, B. Moodley, Preconcentration of molybdenum, antimony and vanadium in gasoline samples using Dowex 1 — x8 resin and their determination with inductively coupled plasma–optical emission spectrometry, Talanta 110 (2013) 153–159.
[36] S. Hirata, T. Kajiya, N. Takano, M. Aihara, K. Honda, O. Shikino, E. Nakayama, Determination of trace metals in seawater by on-line column preconcentration inductively coupled plasma mass spectrometry using metal alkoxide glass immobilized 8-quinolinol, Anal. Chim. Acta. 499 (2003) 157–165.
[37] S. Hirata, Y. Ishida, M. Aihara, K. Honda, O. Shikino, Determination of trace metals in seawater by on-line column preconcentration inductively coupled plasma mass spectrometry, Anal. Chim. Acta. 438 (2001) 205–214.
[38] A. Sabarudin, O. Noguchi, M. Oshima, K. Higuchi, S. Motomizu, Application of chitosan functionalized with 3,4-dihydroxy benzoic acid moiety for on-line preconcentration and determination of trace elements in water samples, Microchim. Acta 159 (2007) 341–348.